Highly Branched Poly(*N*-isopropylacrylamide) for Use in Protein Purification

Steven Carter,[†] Stephen Rimmer,*[,†] Ramune Rutkaite,[†] Linda Swanson,[†] J. P. A. Fairclough,[†] Alice Sturdy,[‡] and Michelle Webb[‡]

The Polymer and Biomaterials Chemistry Laboratories, Department of Chemistry (Polymer Centre), Brook Hill, University of Sheffield, Sheffield, South Yorkshire, S3 7HF, U.K., and Department of Medical Genetics, Centre for Molecular Medicine, University of Manchester, Stopford Building, Manchester M13 9PT

Received December 5, 2005; Revised Manuscript Received January 22, 2006

Poly(*N*-isopropylacrylamide)s with imidazole endgroups were used to separate a histidine-tagged protein fragment directly from a crude cell lysate. The polymers display a lower critical solution temperature that can be tuned to occur at a range of subambient temperatures. UV−visible spectra indicated differences in the binding in aqueous media of Cu(II) and Ni(II) to the imidazole endgroups. These changes in the UV−visible spectra were reflected in the solution/aggregation behavior of the polymers as studied by dynamic light scattering. The addition of Cu(II) disaggregated the polymers, and the polymer coil swelled. On the other hand, when Ni(II) was added the polymers remained aggregated in aqueous media. The polymers were used to purify residues 230−534 of the histidine-tagged breast cancer susceptibility protein his_6−BRCA1. Cu(II) was found to be better suited to the formation of useful polymer−metal ion−protein complexes that display cloud points, since Ni(II)/polymer mixtures generated very little purified protein. The polymers were synthesized using a previously reported variation of the reversible addition−fragmentation chain termination (RAFT) methodology, using the chain transfer agent 3*H*-imidazole-4-carbodithioic acid 4-vinyl benzyl ester with *N*-isopropylacrylamide (NIPAM).

Introduction

The use of poly(*N*-isopropylacrylamide) (PNIPAM) and its copolymers as a thermally responsive polymer is well-documented.[1] In pure water, PNIPAM changes from a coil to a globule conformation at ca. 32 °C.[2] However, the temperature at which the chain conformation changes is dependent on ionic strength.[3−6] The coil-to-globule transition at the lower critical solution temperature (LCST) arises from the entropy gained by the system as hydrogen-bonded water desolvates from the polymer coil. The LCST behavior of these polymers makes for an ideal tool in protein purifications that use thermally induced phase separations to remove specific polymer−protein complexes from crude mixtures of other biomolecules.[7−11] The latter technique uses stimulus-responsive polymers that selectively bind to motifs on the target protein, most commonly histidine tags on recombinant proteins.

In this study, we set out to determine the utility of highly branched polymers with imidazole chain ends to purify a histidine-tagged protein fragment (his_6−BRCA1 230−534) that displays proteolytic and temperature sensitivity. The temperature sensitivity of this species required a polymer with an LCST that was subambient. Control over the LSCT can be achieved by random copolymerization.[12−15] However, the form of the collapsed globule can be influenced by the presence of the comonomer.[16] Alternatively, in architectures that produce segmented monomer sequences, such as block and graft copolymers, and so forth, the LCST tends to be maintained at that of PNIPAM.[17−21] Another way of controlling the LCST is to control the degree of branching.[22,23]

Breast cancer-1, early onset (BRCA1), is a large protein (1863 amino acids) in which mutations are responsible for over 50% of all hereditary breast cancers. Despite the importance of this protein, a detailed mechanistic model for the cellular function of BRCA1 remains elusive, as the protein has proven difficult to isolate in sufficient quantities for the necessary structural and biophysical studies. The development of a functional model will only be facilitated by the purification and characterization of the properties of individual domains/fragments. The soluble his_6−BRCA1 230−534 fragment has previously been purified using Ni(II)−NTA (nitrilotriacetic acid) agarose affinity and ion exchange chromatography.[24] However, because of the proteolytic susceptibility of this protein, this procedure is lengthy, requiring several chromatographic separations to remove the degradation products. Therefore, we have explored the use of water-soluble highly branched imidazole end-functionalized polymers that could be used to obtain pure protein directly from a crude cell lysate preparation.

The binding of transition metal(II) ions to imidazole units in proteins is well-documented[25] and occurs readily in those systems relying on the use of Zn(II), Ni(II), and Cu(II). The use of imidazole groups that have been incorporated into polymers for applications relating to water purification has also been reported for certain polymers.[26] More recently, water-soluble copolymers of *N*-vinylcaprolactam/*N*-vinylimidazole[27] and *N*-isopropylacrylamide/*N*-vinylimidazole[28] have been synthesized to incorporate imidazole units within a linear random copolymer. These polymers rely on the use of the *N*-vinylimidazole as pendant binding units. Galaev et al. have been active in producing imidazole-functional water-soluble polymers based on PNIPAM for use in the purification of histidine-tagged proteins.[10,11] However, they are limited by their molecular architecture and tend to form gels as the number of imidazole binding groups increases. Also, polymers with imidazole groups

* Corresponding author. E-mail: s.rimmer@sheffield.ac.uk. Tel +44 114 222 9565, Fax +44 114 222 9346.
[†] University of Sheffield.
[‡] University of Manchester.

10.1021/bm050929h CCC: $33.50
Published on Web 03/23/2006

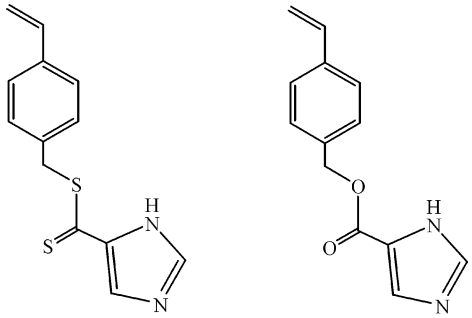

1 **2**

Figure 1. Structures of imidazole dithioate RAFT monomer (**1**) and imidazole ester monomer (**2**).

Table 1. Summary of the NIPAM/1 Feed and NMR Ratios for the Formation of Highly Branched Imidazole Chain-End Functionalized Polymers

feed ratio NIPAM/**1**	mole fraction of **1** in feed (ν)	400 MHz ^{1}H NMR ratio NIPAM/1[a]	mole fraction of **1** in polymer (ν')
25:1	0.040	21:1	0.048
30:1	0.033	28:1	0.036
33:1	0.030	31:1	0.032

[a] The ν values can be used to calculate the mole ratio of imidazole/Cu(II). Thus, for poly(NIPAM-*co*-**1**) ($\nu = 0.040$), the amount of imidazole per gram of polymer can be determined as follows: 1 g = mol(NIPAM) × MW(NIPAM) + mol(**1**) × MW(**1**); where mol(NIPAM) = 21 mol(**1**) so that mol(**1**) = 0.379 mmol·g^{-1} of polymer.

Scheme 1. Synthesis of Imidazole Chain-End Functionalized Highly Branched Polymers from NIPAM and RAFT Agent **1**

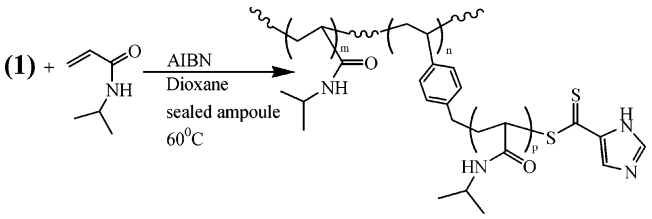

located at the chain ends may be expected to give the maximum exposure of these groups. Thus, the use of highly branched polymers should give improved binding efficiencies and the advantage of higher degrees of functionality. To achieve this, polymers derived from NIPAM and 3*H*-imidazole-4-carbodithioic acid 4-vinyl benzyl ester **1** (Figure 1) can be synthesized using the radical addition fragmentation chain termination (RAFT) methodology,[23] and a summary of the feed ratios of NIPAM/**1** and the associated mole fractions of **1** (ν) that were used in this study are outlined in Table 1. Alternatively, linear versions of these polymers can be synthesized via radical copolymerization of NIPAM and 4(5)-imidazole-(4-vinylbenzyl carboxylate) **2**. The branched polymers, which can be synthesized using the RAFT method as shown in Scheme 1, have the capacity to bind his_6-tagged proteins via metal-mediated complexation at the imidazole chain endgroups.

Experimental Section

Materials. *N*-isopropylacrylamide (Aldrich, 97%) was recrystallized (×3) from hexane (Fisher, HPLC grade) via dissolution at 45 °C then cooling under refrigeration. 4(5)-Imidazoledithiocarboxylic acid (Aldrich, 70%) was used without further purification. α-Azo-bis(isobutyronitrile) (AIBN) (BDH, 97%) was recrystallized from diethyl ether (Fisher, HPLC grade). *N*,*N*-Dimethylformamide (DMF) (Aldrich, sure-seal) and dioxane (Aldrich, sure-seal) were used as purchased. Copper-(II) sulfate pentahydrate (Sigma, 99.7%) and nickel(II) chloride hexahydrate (Sigma) were used as received. Sodium chloride (Fisher) was used as supplied. Acrylamide/*N*,*N*′-methylene bisacrylamide (Bio-Rad), *N*,*N*,*N*,*N*-tetramethylethylenediamine (Sigma), tris(hydroxymethy)methylamine (Sigma), ammonium peroxysulfate (BDH), glycine (BDH), and sodium dodecyl sulfate (SDS) (Sigma) were used as supplied for the sodium dodecyl sulfate polyacrylamide gel electrophoresis (SDS PAGE) analysis.

Instrumentation. ^{1}H NMR (400 MHz) spectra were recorded using a Bruker AMX2-400 instrument. Optical density measurements of aqueous solutions of polymers were performed using a Varian Cary 3Bio UV−visible spectrometer. The temperature of the cell holder was controlled with a Varian Cary temperature controller to an accuracy of ±0.1 °C. Deionized water was obtained from a Millipore (Milli-Q) purification system at resistivity of 18.2 MΩ cm. SDS polyacrylamide gels were electrophoresed in mini-protean III gel tanks (BioRad) at 40 mA using a Power Pac 300 (BioRad). Ultrafiltration was carried out using a 300 cm^3 stirred cell (Millipore, U.K.) at 400 kPa nitrogen pressure with 70 mm cellulose 10 000 MWCO filters (Millipore, U.K.). Centrifugation was carried out on a Beckman Allegra X-22 centrifuge equipped with a swing-bucket (SX4250) rotor. DLS data were collected using a Brookhaven BI-200SM goniometer, equipped with an avalanche photodiode (APD) and a 35 mW He−Ne laser (633 nm). Analysis was performed using the CONTIN method.

Synthesis and Purification of Copolymers of NIPAM with 1, (poly(NIPAM-*co*-1). The polymerization of NIPAM with **1** was carried out according to a previously reported procedure.[23] Thus, for the formation of poly(NIPAM-*co*-**1**) where the mole fraction of **1**, $\nu =$ 0.029, NIPAM (3.514 g, 30.9 mmol) was dissolved in dioxane (11 cm^3) and added to the required amount of **1** (0.94 mmol, 245 mg). The initiator, AIBN (0.94 mmol, 152 mg) was then dissolved in the solution. Similarly, for the formation of poly(NIPAM-*co*-**1**) where the mole fraction of **1**, $\nu = 0.033$, NIPAM (3.514 g, 30.9 mmol) was dissolved in dioxane (11 cm^3) and added to the required amount of **1** (1.03 mmol, 268 mg), and AIBN (0.94 mmol, 152 mg) was dissolved in the solution. The solutions were then transferred to glass ampules, polymerized, and purified according to the reported procedure. The polymers were obtained as orange solids in final yields of 18−20%. The structure of the polymers was confirmed by ^{1}H NMR spectroscopy[23] (the key resonances are δ 6.7−8.0, aryl Hs from xylyl and imidazole; δ 4.0, $(CH_3)_2CH^*-$; and δ 0.9, $(CH_3^*)_2CH-$). The weight average molecular weights of the polymers were 23.0 ($\nu = 0.029$) and 24.7 kg mol^{-1} ($\nu = 0.033$) as determined by GPC in DMF (0.01% ammonium acetate) eluant.[23] The degree of branching (number of branches per repeat unit) found from ^{1}H NMR spectra[23] were 0.15 ($\nu = 0.033$) and 0.08 ($\nu = 0.029$).

The linear analogous polymers, prepared by copolymerization of NIPAM with **2** were prepared as previously desribed.[23]

Preparation of Polymer-Protein conjugates. *Preparation of Polymer−Cu(II) and Polymer−Ni(II) Complexes.* The polymer (100 mg) was dissolved in deionized water (5.0 cm^3) by solubilizing at 0−1 °C over ice. Aqueous $Cu(II)SO_4$ (0.1 mol dm^{-3}, 2.0 cm^3) was added and the solution made saline by dissolution of NaCl (327.3 mg, 5.60 mmol). A polymer−Ni(II) complex was similarly prepared using aqueous $Ni(II)Cl_2$ (0.1 mol dm^{-3}, 2.0 cm^3). Each solution was allowed to warm to room temperature (ca. 20 °C), centrifuged at 20 °C (2756 g, 10 min), and the supernatant decanted off. The solids were redissolved in aqueous 800 mmol dm^{-3} NaCl (5.0 cm^3) at 0−1 °C and allowed to reprecipitate at 20 °C, then centrifuged. The process was repeated so that a total of three precipitations/separations had been carried out. The polymer−Cu(II) and polymer−Ni(II) complexes were each finally redissolved in aqueous NaCl (800 mmol dm^{-3}, 5.0 cm^3) at 0−1 °C and stored for 16 h at 4 °C before use.

Purification of BRCA1 Protein from Crude Lysate using Ni(II) and Cu(II) Polymer−Metal Complexes. A solution of the polymer−metal-(II) complex (approximately 20 mg cm^{-3}) in aqueous NaCl (800 mmol dm^{-3}, 5.0 cm^{-3}) was incubated with the cell lysate containing his_6−

BRCA1 230−534 in a solution of aqueous Tris−HCl buffer (20 mmol dm^{-3}, pH 7.5)/NaCl (800 mmol dm^{-3}, 3.0 cm^{-3}) with a complete protease inhibitor tablet, then gently agitated at 0−1 °C for 30 min. The solution was precipitated by incubation at 18−19 °C, then centrifuged at 20 °C (2756 g, 5 min). The supernatant was removed and stored at 0−1 °C. The precipitant was washed with an ice-cold mixture of aqueous Tris−HCl buffer (20 mmol dm^{-3}, pH 7.5)/ NaCl (800 mmol dm^{-3}, 5.0 cm^3), then redissolved in the same buffer at −10 °C over 30 min. The polymer was allowed to precipitate again, and the procedure was repeated twice. his_6−BRCA1 230−534 was eluted by redissolving the final precipitate in the aqueous Tris−HCl (20 mmol dm^{-3}, pH 7.5)/NaCl buffer (800 mmol dm^{-3}) containing imidazole (300 mmol dm^{-3}, 5.0 cm^3) at 0−1 °C and then warming to 18−19 °C. The whole sample was centrifuged in order to remove the solids, then the supernatant eluant was retained and stored at 0−1 °C.

Dynamic Light Scattering. Aqueous polymer solutions (10 mg cm^{-3}) were prepared by dissolving the polymer (25 mg) in water (2.5 cm^3) at 0−1 °C, then filtering through a 2-μm filter directly into a clean glass cuvette. The copper(II) and nickel(II) complexed polymer samples at a concentration of 3.85 mmol dm^{-3} were formed via the addition of either 0.1 M copper(II) sulfate (100 μL) or 0.1 M nickel-(II) chloride (100 μL), then allowed to equilibrate at 0−1 °C for 5 min prior to filtration.The sample was then stoppered and placed in the laser beam of the DLS instrument. The sample was in thermal contact with a Decalin bath, which was heated in a stepwise manner in the range 17−24 °C. The heating was performed via a water bath that heats brass plates above and below the Decalin, as such a temperature difference exists between the water bath and the Decalin. For this reason, the sample temperature is measured in the Decalin by a PRT (platinum resistance thermometer).

UV−visible Spectroscopy. Aqueous polymer solutions (1 mg cm^{-3}) were prepared by dissolving the polymer in water at 0−1 °C. An aliquot of either Cu(II)SO_4 (100 mmol dm^{-3}) or Ni(II)Cl_2 (100 mmol dm^{-3}) was then added to the sample to obtain the desired concentration of metal ions, and the solution was allowed to equilibrate for 5 min. The UV−visible spectra were then recorded at room temperature in the 1000−200 nm range.

Determination of Solution Turbidity. The lower critical solution temperature (LCST) of aqueous solutions of the polymers were obtained from optical density measurements at a concentration of 1 mg cm^{-3} in deionized water. Aliquots of aqueous Cu(II)SO_4 (100 mmol dm^{-3}) were added to separate samples of the aqueous polymer solutions to give the appropriate concentration of Cu(II) ions, then allowed to equilibrate for 5 min. The change in optical density was then monitored as a function of temperature (5−45 °C or 5−60 °C, heating rate 0.5 °C min^{-1}) at a fixed wavelength of 500 nm. The cloud points were determined as the temperature at which the point of inflection of the increase in absorbance occurred upon raising the temperature of the sample. The accuracy of the values was determined as ±0.5 °C.

Effect of Ionic Strength on LCST of poly(NIPAM-*co*-1) (ν = 0.033). The lower critical solution temperatures (LCST) of the branched poly(NIPAM-*co*-**1**)(ν = 0.033) polymer was determined at increasing sodium chloride concentrations using optical density measurements at a concentration of 1 mg cm^{-3}. The polymer (10 mg) was dissolved in water (1.0 cm^3) at 0−1 °C (ice-bath), and the appropriate amount of sodium chloride was dissolved in the solution to give a concentration range of 10−1000 mmol dm^{-3}. The solution was diluted with water (×10); then, the LCST was recorded, and the sample then recooled to attain dissolution of the polymer. An aqueous Cu SO_4 solution (100 mmol dm^{-3}) was diluted with water (×10), then 50 μL of this solution was added to the aqueous polymer solution to form the polymer−Cu-(II) complex (0.5 mmol g^{-1} polymer), and the LCST was re-recorded. The change in optical density was monitored as a function of temperature (5−45 °C, heating rate 0.5 °C min^{-1}). The accuracy of the values was determined as ±0.5 °C.

Preparation of His_6−BRCA1 230−254 Containing Cell Lysates. His_6−BRCA1 230−534 was produced from the expression vector pET 22b in the *E. coli* BL21 DE3 codon plus. For comparative analysis of the different polymer metal complexes, a 500 cm^{-3} culture, expressing his_6−BRCA1 230−534, was divided into 100 cm^{-3} fractions and cell lysate prepared from each, following published procedures.[24] This ensured that the initial amounts of his_6−BRCA1 230−534 to be purified by each polymer metal complex were identical.

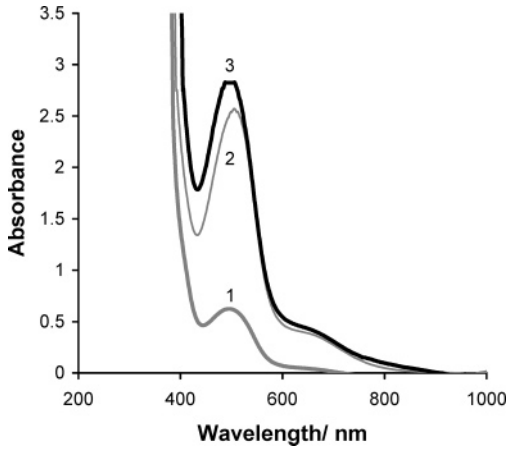

Figure 2. UV−vis absorbance spectrum of an aqueous solution of poly(NIPAM-*co*-**1**) (ν = 0.040) at increasing concentrations of copper-(II) sulfate: 1, 0.03 mmol dm^{-3}; 2, 0.2 mmol dm^{-3}; 3, 0.8 mmol dm^{-3}. The polymer concentration is 1 wt %. Spectra were recorded after 5 min following addition of the $CuSO_4$.

SDS PAGE Analysis. Samples containing his_6-BRCA1 230−534 were made up in glycerol (1 mol dm^{-3}), SDS (100 mmol dm^{-3}), bromophenol blue (0.0125 wt %), Tris−HCl (60 mmol dm^{-3}), and DTT (5 mmol dm^{-3}), heated to 95 °C for 5 min, and analyzed in 15% SDS polyacrylamide gels. The gels were electrophoresed at 40 mA toward the cathode until the bromophenol blue had reached the bottom of the gel. Proteins were visualized by Coomassie blue staining and analyzed by comparison to standard molecular weight markers.

Results and Discussion

UV-visible Spectroscopy and Cloud-Point Studies on Polymer−Cu(II) and Polymer−Ni(II) Complexes. The effect of adding increasing amounts of Cu(II)SO_4 to the imidazole chain end-functionalized highly branched polymer, poly(NIPAM-*co*-**1**) (ν = 0.040) was monitored by UV−visible spectroscopy. An absorption peak characteristic of Cu(II) imidazole binding was observed at ca. 500 nm. The addition of increasing amounts of Cu(II)SO_4 to the solution produced an increase in the intensity of this peak, as illustrated in Figure 2. The formation of the complex was not immediate but occurred over a 60 min period, as evidenced by UV−visible measurements (see insert in Figure 2), which showed a gradual increase in the intensity of the 500 nm absorbance peak over this period with a corresponding color change from yellow to orange. As there was no apparent change in the profile of the absorption, as evidenced by the UV−visible measurements, the change in color appears to arise from the increasing number of imidazole groups that become bound to Cu(II) ions. Also, an increase in the intensity of this adsorption did not occur beyond a concentration of $CuSO_4$ of 0.8 mmol dm^{-3}, indicating that this is the maximum amount of Cu(II) ions that can be specifically bound to the imidazole chain endgroups. At this point, the imidazole groups appear to be fully saturated with Cu(II) ions, and the amount of Cu(II) ions that bind to the polymer was calculated to be 0.143 mmol g^{-1}. ^1H NMR spectra indicate that this approximates to a mole ratio of imidazole/Cu of 2:1 (see footnote, Table 1). The latter stoichiometry is in agreement with the reported stoichiometry of the

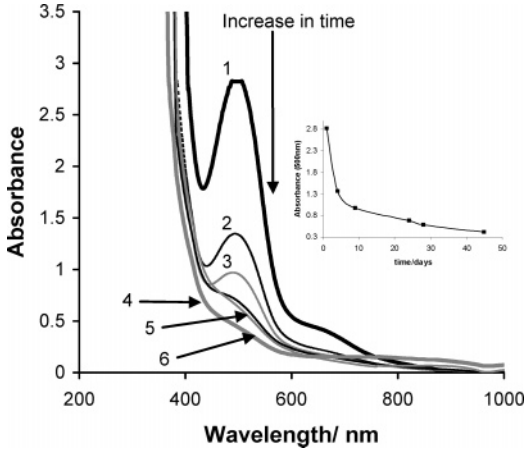

Figure 3. UV−vis absorbance spectrum of an aqueous solution of poly(NIPAM-*co*-**1**) ($\nu = 0.040$) showing stability of the Cu(II)−imidazole complex at room temperature at extended times: 1, after 1 day; 2, 4 days; 3, 9 days; 4, 24 days; 5, 28 days; 6, 45 days. Insert graph shows evolution of absorbance maxima (A_{500}) with extended time. The $CuSO_4$ concentration in the solution was 0.8 mmol dm^{-3}, and the polymer concentration 1 wt %.

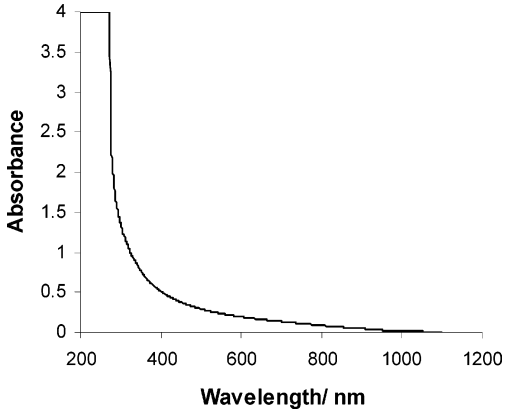

Figure 4. UV−vis absorbance spectrum of an aqueous solution of poly(NIPAM-*co*-**2**) ($\nu = 0.040$) at $Cu(II)SO_4$ concentration of 0.8 mmol dm^{-3}. The polymer concentration is 1 wt %.

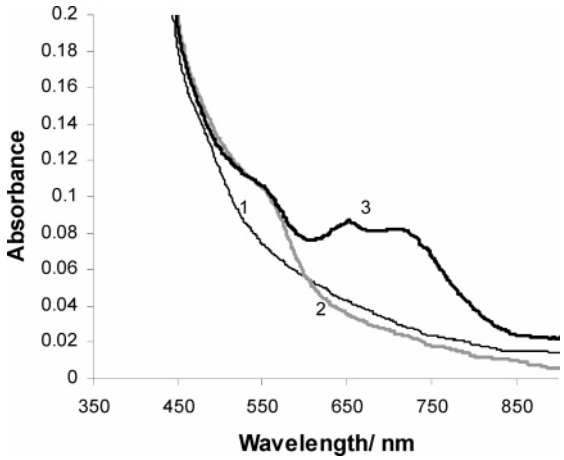

Figure 5. UV−vis absorbance spectra of the aqueous solution of poly(NIPAM-*co*-**1**) ($\nu = 0.040$) in the presence of increasing amounts of $NiCl_2$ (2.7 mmol dm^{-3}): 1, 0.27 mmol dm^{-3}; 2, 2.7 mmol dm^{-3}; 3, 27 mmol dm^{-3}. The polymer concentration is 1 wt %. Spectra were recorded after 5 min following addition of the $NiCl_2$.

solid-state structure imidazole-4-thiocarboxylic acid−Cu(II) complexes: the closest low molecular analogues available in the literature.[29] These authors concluded that the imidazole-4-thiocarboxylic acid−Cu(II) had a square planar arrangement between one Cu(II) atom and two of the imidazole dithioate groups and that the binding occurs via the N(1) atom of imidazole and the S atom of the C═S bond. Since we observe the same stoichiometry, we can tentatively suggest the polymer complexes described here probably have a structure that is similar to the low molecular weight analogues. The stability of the complex at room temperature was determined by assessing the intensity of the absorbance at 500 nm. It was found that the complex was stable up to 24 h; no changes in the form or intensity of the adsorption were observed. However, at times longer than 24 h, the complex became unstable, as shown in Figure 3, whereupon it was observed to change color from orange through to yellow up to 48 h. It would thus appear that the binding of Cu(II) ions to the imidazole chain endgroups of the highly branched polymer results in a complex that is stable for up to 24 h. Since it would not normally be expected that an imidazole−Cu(II) complex would become unstable at extended times, the instability is probably due to the involvement of the dithionate ester. However, further work is needed to fully define the structure(s) and stabilities of these chain-end complexes.

The linear PNIPAM with pendant imidazole carboxylate groups formed from NIPAM and **2** ($\nu = 0.040$, $\nu' = 0.044$),[23] in the presence of 0.8 mmol dm^{-3} Cu(II) ions, has the UV−visible spectrum shown in Figure 4. It would appear that the only significant region is at 200−300 nm due to aromatic absorption, and no specific absorbance was observed at 500 nm. Thus, if we assume that the linear polymer also forms a Cu(II)−imidazole complex, we can propose that the complex formed from the endgroups derived from the RAFT polymerization involves ligation by the sulfur groups of the dithionate ester as well as the imidazole groups.

The binding of $Ni(II)Cl_2$ to the imidazole chain end-functionalized highly branched polymer, poly(NIPAM-*co*-**1**) ($\nu = 0.033$), was also monitored by UV−visible spectroscopy and gave the spectrum shown in Figure 5. The absorbance at $\lambda = 560$ nm was only observed at high concentrations of Ni(II) (at least 2.7 mmol dm^{-3}). Also, at higher concentrations (27 mmol dm^{-3}), an additional absorbance peak centered at 680 nm was observed, which may be attributed to $[Ni(H_2O)_6]^{2+}$ ions and/or $[Ni(H_2O)_{6-n}Cl_n)^{30}$ ions at high concentrations of Ni(II) chloride. Thus, the metal(II) ion spectra, while not offering unequivocal structural information, do indicate the ease with which Cu(II)−highly branched PNIPAM complexes can be formed in comparison to the Ni(II)−highly branched PNIPAM complexes, while it can be shown that the linear analogues of these complexes do not display the same binding characteristics.

The effect of Cu(II) ions on the polymer cloud point was explored by determining the change in solution turbidity with temperature upon the addition of increasing amounts of Cu(II) ions. The data shown in Figure 6 for the poly(NIPAM-*co*-**1**) shows that the addition of Cu(II) ions, at concentrations of 0.03 and 0.2 mmol dm^{-3}, increased the cloud point to a temperature above 60 °C, which was the highest temperature studied. However, when the concentration was increased to 0.8 mmol dm^{-3}, a cloud point was observed, as an increase in turbidity at 37 °C, which is considerably higher than the cloud point of the noncomplexed polymer (12−15 °C).

Therefore, the effect of adding Cu(II) ions is to initially increase the LCST and then as the concentration is increased further to decrease the LCST. Thus, there appear to be at least two processes that must be considered to explain these data. We previously reported that the LCST of branched PNIPAMs with imidazole endgroups are lower than equivalent linear polymers, in which the imidazole groups are placed along the

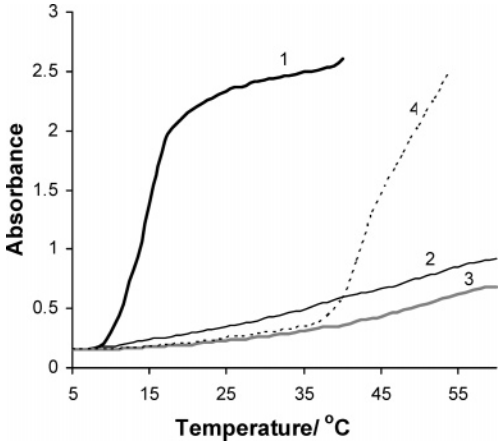

Figure 6. Optical density of the aqueous solution of poly(NIPAM-*co*-**1**) ($\nu = 0.039$) (0.56 wt %) as a function of the temperature at different concentrations of $CuSO_4$: 1, 0 mmol dm^{-3}; 2, 0.03 mmol dm^{-3}; 3, 0.2 mmol dm^{-3}; 4, 0.8 mmol dm^{-3}. Heating rate 0.5 °C/min, observation at 500 nm. Measurements were recorded after 5 min following addition of the $CuSO_4$.

Table 2. Dynamic Light Scattering Results for Poly(NIPAM-*co*-**1**) ($\nu = 0.033$) Showing the Effect of Cu(II) and Ni(II) Ions

	particle size/nm		
temperature/°C	native	Ni(II)	Cu(II)
17	15 (±4), 48 (±6)	14 (±1), 70 (±5)	53 (±1)
20	15 (±4), 44 (±6)	14 (±1), 30 (±2)	53 (±1)
24	15 (±4), 44 (±6)	52 (±1)	92 (±2)

main chain.[23] We also proposed that the decrease in LCST as the degree of branching increased could be explained by assuming that the chain-end imidazole groups aggregate to a greater degree than the pendant imidazole groups on the linear polymers. The addition of Cu(II) then dissociates these aggregates as the Cu(II)−imidazole complexes form. These complexes are much more polar then the imidazole aggregates so that the LCST increases above the maximum recorded temperature of 60 °C. However, the other effect of adding Cu(II)SO_4 is to increase the ionic strength of the system. The increase in ionic strength tends to decrease the LCST, and at a Cu(II) concentration of 0.8 mmol dm^{-3}, the LCST is observed at 37 °C (see the section on the effect of ionic strength).

Dynamic Light Scattering Study on Metal-Complexed Polymers. The polymer coiling−aggregation effects of poly(NIPAM-*co*-**1**) ($\nu = 0.033$) in water were examined using dynamic light scattering (DLS). The technique allowed the effect of Cu(II) and Ni(II) on the coil comformation and polymer aggregation effects of this polymer to be explored. An aqueous solution of the polymer at a concentration of 10 mg cm^{-3} was observed to have a bimodal distribution of particle sizes[28] of 15 and 44 or 48 nm (Table 2) in the temperature range 17−24 °C, which was below the cloud point of the polymer. In the presence of Ni(II) ions, a bimodal distribution was again observed with a similar range of particle sizes of 14 and 70 or 30 nm. However, in the presence of Cu(II) ions, the polymer showed a predominantly unimodal distribution ranging from 33 to 92 nm (average 53 nm). These observations can be tentatively interpreted as follows. It would thus appear that Cu(II) ions have the effect of binding to the imidazole functionality located at the polymer chain-ends, while the Ni(II) ions do not have this capacity. The polymer is normally present in water as an average bimodal distribution of aggregates (15 and 48 nm). The disruption of these aggregates into polymer coils is made possible by Cu(II) ions but not Ni(II) ions. Cu(II) ions are able to bind more strongly to imidazole chain ends, rendering the polymer more hydrophilic. Therefore, when the aggregates are disrupted into a distribution of polymer chains or aggregates of smaller dimensions, the Cu(II) ions have the effect not only of causing this disruption to now form an average monomodal distribution but also of expanding the polymer coils to dimensions up to 92 nm. The swelling of the polymer coils is thus associated with loss of aggregation. These results also reinforce the observations from the cloud-point studies that the effect of Cu(II) ions is to disrupt the polymer aggregation caused by binding between imidazole groups. The subsequent swelling of the polymer chains by Cu(II) ions appears to be an effect that can be directly observed from DLS studies. Thus, it can be clearly seen by reference to Table 2 that addition of Ni(II) had little or no effect on the overall size of the polymer aggregates, whereas addition of Cu(II) had the marked effect of increasing the hydrodynamic size of the polymer in aqueous media and creating a unimodal distribution of coil sizes.

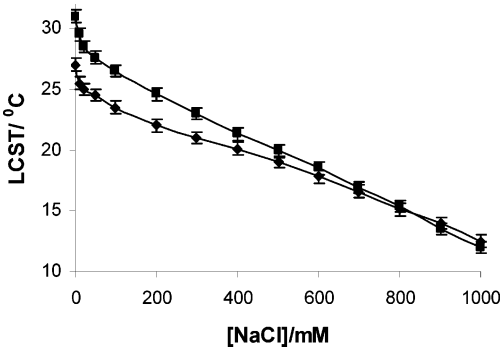

Figure 7. Effect of NaCl on cloud point of aqueous solution of poly(NIPAM-*co*-**1**) ($\nu = 0.033$) polymer (◆, native; ■, in the presence of Cu(II)).

Effect of Ionic Strength on Cloud Point. Ionic strength is a key variable in many applications in biotechnology. However, only a few authors appear to have considered this aspect.[4−6] The change in the cloud point with increasing ionic strength (sodium chloride concentration) was determined for a highly branched poly(NIPAM-*co*-**1**) ($\nu = 0.033$), in order to obtain a sodium chloride concentration that would give an LCST low enough, and therefore suitable, for protein extraction experiments. Figure 7 shows that the LCST decreased continuously when the NaCl concentration was increased from 10 mmol dm^{-3} to 1 mol dm^{-3} in aqueous solution. Figure 7 also compares the effect of increasing ionic strength on solutions of a noncomplexed polymer and on the Cu(II)−polymer complex. In the presence of Cu(II) ions, the decrease of LCST is almost identical to that observed with the noncomplexed polymer. At concentrations of NaCl above 600 mmol dm^{-3}, the LCSTs of the Cu(II)−polymer complex were not significantly different from the solution of the polymer in the absence of Cu(II). However, below this concentration, the LCST is lower for the noncomplexed polymer. Thus, a convergence point was reached where in the presence of increasing amounts of NaCl the cloud points of both the noncomplexed polymer and the Cu(II)−polymer complex solutions were essentially equivalent.

Purification of Histidine-Tagged Proteins. The purification of proteins using affinity chromatography has proven particularly useful for the separation of proteins that have been fused to a run of histidine residues at either their N or C termini. Here, we report a procedure for the one-step purification of a his_6−BRCA1 230−534 protein directly from a cell lysate using Cu(II)-mediated protein binding.[22] The process, as outlined in Scheme 2, involved forming a polymer−metal complex by

Scheme 2. Cu(II)-Mediated Affinity Precipitation of His_6−BRCA1 Showing Initial Binding to His_6-Tag, Polymer Coil Collapse upon Raising Temperature, and Subsequent Release of Protein.

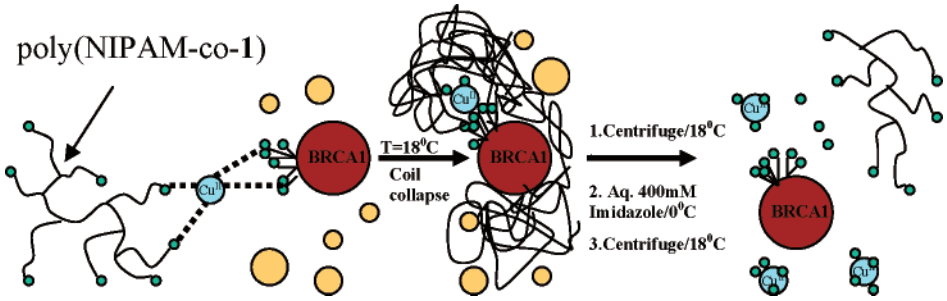

binding the imidazole units at the polymer chain ends to Cu(II) ions. This complex binds to the protein at the his_6 tag via Cu(II) ions at low temperature (0−1 °C) to form a polymer−protein complex,[11] and upon raising the temperature was precipitated and separated from the cell lysate. This process was repeated to ensure that nonspecifically bound protein is removed, then monomeric imidazole was added to the polymer−protein complex to release the his_6-tagged protein.

The affinity precipitation of his_6−BRCA1 230−534 was carried out using Cu(II)-mediated his-tagged binding to the imidazole chain end highly branched polymer. The protein fragment had previously been separated using conventional techniques, namely, diethylaminoethyl (DEAE) ion exchange chromatography and a commercially available Ni(II)−NTA affinity column. This procedure can normally be carried out at low temperature. However, it requires intermediate purification steps before the final purification using the NTA column and is a relatively lengthy procedure. In contrast, we were able to carry out binding experiments directly from cell lysates.

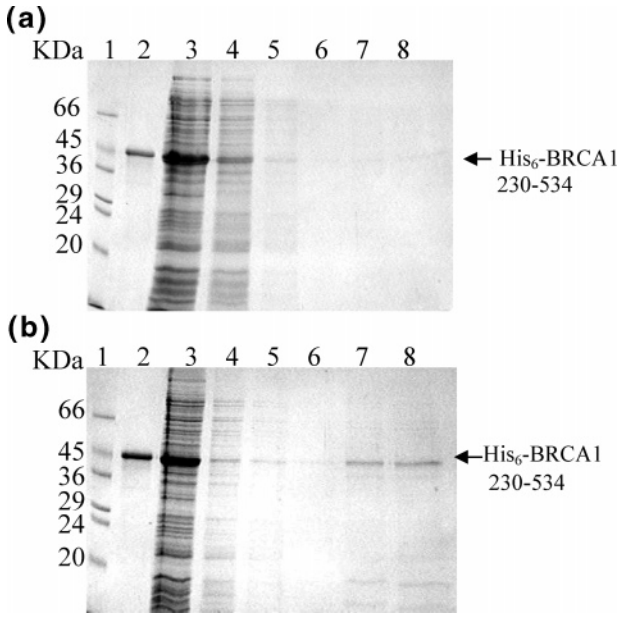

Figure 8. Purification of his_6−BRCA1 230−534 by affinity precipitation at 22−25 °C using imidazole-functionalized poly(NIPAM-*co*-**1**) ($\nu = 0.029$): (a) Ni(II) chelated and (b) Cu(II) chelated**.** In both, lane 1 contains molecular weight markers; lane 2, his_6−BRCA1 230−534 purified by Ni(II) NTA and ion exchange chromatography;[21] lane 3, his_6−BRCA1 230−534 containing cell lysate; lane 4 unbound after incubation with poly(NIPAM-*co*-**1**) ($\nu = 0.029$) polymer−metal(II) complex; lanes 5 and 6 are washes 1 and 2, respectively; and lanes 7 and 8 are fractions eluted with 20 mM Tris pH 7.5, 800 mM NaCl, 300 mM imidazole. Gels were visualized by Coomassie blue staining and analyzed by comparison to molecular weight markers and purified his_6−BRCA1 230−534.

The procedure used both Ni(II) and Cu(II) ions with an imidazole end-functionalized polymer formed using poly(NIPAM-*co*-**1**) **(**$\nu = 0.029$**)**. The polymer−metal complexes were formed by the addition of aqueous $Ni(II)Cl_2$ and $Cu(II)SO_4$ to aqueous polymer solutions and removing excess metal via the process of precipitation/centrifugation. The aqueous solutions of polymer−metal complexes were then incubated with the crude cell lysate ($[Cu(II)] = 0.8$ mmol dm^{-3}), to allow binding to BRCA1 230−534. The procedure could be carried out using polymer concentrations high enough to allow sufficient protein binding to take place (ca. 15 mg cm^{-3}) but not so high as to introduce gelation effects that could be observed at concentrations above 20 mg cm^{-3} and which may retard polymer/protein diffusion.

Eluted fractions containin purified BRCA1 230−534 were analyzed by SDS polyacrylamide gels by comparison to a protein purified by Ni(II)−NTA and ion exchange chromatography[24] and using molecular weight standards as points of reference. It was found that high levels of purification could be obtained using Cu(II) ions whereas very little his_6-BRCA1 230−534 could be obtained using a similar system incorporating Ni(II) ions. The SDS PAGE gels from these extractions are shown in Figure 8a,b.

This observation indicates that the binding of his_6−BRCA1 230−534 via Ni(II) to the polymer either forms a more stable complex than with Cu(II), which cannot be as easily eluted in the presence of imidazole, or the Ni(II) ions do not facilitate the binding of the his-tagged protein to the metal−polymer complex. This latter effect may be supported by comparing the UV−visible data in Figures 2 and 5, which shows that the highly

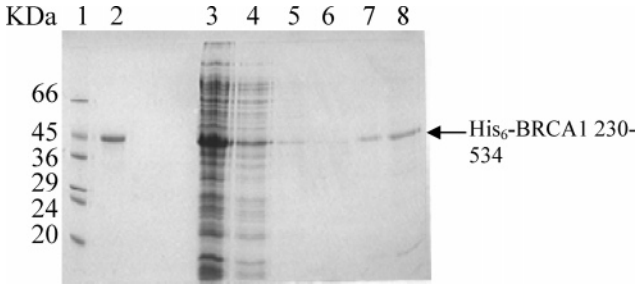

Figure 9. Purification of his_6−BRCA1 230−534 by affinity precipitation at 17−19 °C using imidazole-functionalized poly(NIPAM-*co*-**1**) ($\nu = 0.033$) chelated with Cu(II). Lane 1 contains molecular weight markers; lane 2, his_6−BRCA1 230−534 purified by Ni(II) NTA and ion exchange chromatography;[21] lane 3, his_6−BRCA1 230−534 containing cell lysate; lane 4 unbound after incubation with poly(NIPAM-*co*-**1**) ($\nu = 0.033$) polymer−metal (II) complex; lanes 5 and 6 are washes 1 and 2, respectively; and lanes 7 and 8 are fractions eluted with 20 mM Tris pH 7.5, 800 mM NaCl, 300 mM imidazole. Gels were visualized by Coomassie blue staining and analyzed by comparison to molecular weight markers and purified his_6−BRCA1 230−534.

branched imidazole chain-end polymers form complexes with Cu(II) ions that absorb in the visible region of the spectrum.

When using poly(NIPAM-*co*-**1**) ($\nu = 0.029$)**,** precipitation occurred close to room temperature (24−25 °C). However, we were able to improve the process by using poly(NIPAM-*co*-**1**) ($\nu = 0.033$), which has a lower LCST, and this material allowed us to precipitate the protein at 17−19 °C. Figure 8b shows that the precipitations carried out at 24−25 °C were susceptible to proteolytic fragmentation of the BRCA1 230−534. Clearly, several proteolytic fragments were observed as shown by the presence of bands at ca. 36kDa and below 20 kDa. However, the precipitations at 17−19 °C, using poly(NIPAM-*co*-**1**) ($\nu = 0.033$), gave lower extents of proteolytic degradation, as shown in Figure 9.

Conclusions

We have shown that highly branched PNIPAMs with imidazole endgroups are useful materials for temperature-dependent precipitation of an important recombinant protein fragment. Improved separation with lower degrees of proteolytic fragmentation could be achieved by using polymers that can form protein complexes that precipitate at 17−19 °C rather than polymers that require the use of higher precipitation temperatures. The LCST of the branched PNIPAMs was also shown to be dependent on both Cu(II) concentration and on the overall ionic strength. The presence of Cu(II) in solution affects the state of aggregation of the chain in aqueous media. That is, dynamic light scattering measurements show that in the absence of Cu(II) the highly branched PNIPAMs with imidazole endgroups form aggregated structures. The structures disaggregate as Cu(II) is added as the polymer coil swells. On the other hand, the light scattering measurements show that as Ni(II) is added to the same polymer solutions the polymer coils remain aggregated. Differences between the Cu(II) and Ni(II) complexes are also observed in the visible spectra of the solutions, and we propose that these differences are due to a greater affinity for the Cu(II) ions due to ligation by the dithionate ester as well as the imidazole group of the endgroups derived from the RAFT agent. These structural differences appear to influence the performance of these polymers in the purification of a his-tagged recombinant protein: Purifications with the Cu(II) complexes were more successful then attempts at purification with the Ni-(II) complexes.

Acknowledgment. The authors would like to thank BBSRC and EPSRC for their support of this work in the form of postdoctoral fellowships for Steven Carter and Ramune Rutkaite and a Ph.D. studentship for Alice Sturdy.

References and Notes

(1) Gil, E. S.; Hudson, S. M. *Prog. Polym. Sci.* **2004**, *29*, 1173.
(2) Heskins, M.; Guillet, J. E. *J. Macromol. Sci. Chem.* **1968**, *8*, 1441.
(3) Liu, X.-M.; Wang, L.-S.;Wang, L.; Huang, J.; He, C. *Biomaterials* **2004**, *25*, 5659.
(4) Chen, G.; Hoffman, A. S. *Macromol. Chem. Phys.* **1995**, *196*, 1251.
(5) Park, T. G.; Hoffman, A. S. *Macromolecules* **1993**, *26*, 5045.
(6) Chen, J. P.; Yang, H. J.; Hoffman, A. S. *Biomaterials* **1990**, *11*, 625.
(7) Kumar, A.; Galaev, I. Yu.; Mattiasson, B. *Biotechnol. Bioeng.* **1998**, *59*, 695.
(8) Kumar, A.; Galaev, I. Yu.; Mattiasson, B. *Bioseparation* **1999**, *7*, 185.
(9) Kumar, A.; Galaev, I. Yu.; Mattiasson, B. *Bioseparation* **1998**, *7*, 129.
(10) Kumar, A.; Khalil, A. A. M.; Galaev, I. Yu.; Mattiasson, B. *Enzymol. Micro. Technol.* **2003**, *33*, 113.
(11) Kumar, A.; Kamihira, M.; Galaev, I. Yu.; Mattiasson, B. *Langmuir* **2003**, *19*, 865.
(12) Spafford, M.; Polozova, A.; Winnick, F. M. *Macromolecules* **1998**, *31*, 1, 7099.
(13) Kurisawa, M.;Yokayama, M.; Okano, T. *J. Controlled Release* **2000**, *69*, 127.
(14) Tiera, M.; dos Santos, G. R.; de Oliveira Tiera, V. A.; Vieira, N. A. B.; Frolini, E.; da Silva, R. C.; Loh, W. *Colloid Polym. Sci.* **2005**, *283*, 662.
(15) Chee, C. K.; Rimmer, S.; Shaw, D. A.; Soutar, I.; Swanson, L. *Macromolecules* **2001**, *34*, 7544.
(16) Barker, I. C.; Cowie, J. M. C.; Huckerby, T. N.; Shaw, D. A.; Soutar, I.; Swanson, L. *Macromolecules* **2003**, *36*, 7765.
(17) Chilkoti, A.; Chen, G.; Stayton, P. S.; Hoffman, A. S. *Bioconjugate Chem.* **1994**, *5*, 504.
(18) Hoffman, A. S.; Stayton, P. S. *Macromol. Symp.* **2004**, *207*, 139.
(19) Schilli, C. M.; Zhang, M.; Rizzardo, E.; Thang, S. H.; Chong, Y. K.; Edwards, K.; Karlsson, G.; Muller, A. H. E. *Macromolecules* **2004**, *37*, 7861.
(20) Durand, A.; Hourdet, D. *Polymer* **1999**, *40*, 4941.
(21) Bokias, G.; Mylonas, Y.; Staikos, G.; Bumbu, G. G.; Vasile, C. *Macromolecules* **2001**, *34*, 4958.
(22) Carter, S.; Rimmer, S.; Sturdy, A.; Webb, M. *Macromol. Biosci.* **2005**, *5*, 5373.
(23) Carter, S.; Hunt, B.; Rimmer, S. *Macromolecules* **2005**, *38*, 4595.
(24) Sturdy, A.; Naseem, R.; Webb, M. *J. Mol. Biol.* **2004**, *340*, 469.
(25) Glusker, J. P. *Adv. Protein Chem.* **1991**, *42*, 1.
(26) Molina, M. J.; Gomez-Anton, M. R.; Rivas, B. L.; Maturana, H. A.; Pierola, I. F. *J. Appl. Polym. Sci.* **2000**, *79*, 1467.
(27) Lozinsky, V. I.; Simenel, I. A.; Kulakova, V. K.; Kuskaya, E. A.; Babushkina, T. A.; Klimova, T. P.; Burova, T. V.; Dubovik, A. S.; Grinberg, V. Y.; Galaev, I. Yu.; Mattiasson, B.; Khokhlov, A. R. *Macromolecules* **2003**, *36*, 7308.
(28) Wahlund, P.-O.; Galaev, I. Yu.; Kazakov, S. A.; Lozinsky, V. I.; Mattiasson, B. *Macromol. Biosci.* **2002**, *2*, 33.
(29) Kondo, M.; Shimizu, E.; Horiba, T.; Tanaka, H.; Fuwa, Y.; Nabari, K.; Unoura, K.; Naito, T.; Maeda, K.; Uchida, F *Chem. Lett.* **2003**, *32*, 944.
(30) Miyaji, K.; Nozawa, K.; Morinaga, K. *Bull. Chem. Soc. Jpn.* **1989**, *62*, 1472.

BM050929H